Inorganic Chemistry

Article

pubs.acs.org/IC

Characterization of the Hydrides in Stryker's Reagent: $[HCu\{P(C_6H_5)_3\}]_6$

Elliot L. Bennett,[†] Patrick J. Murphy,[†] Silvia Imberti,[‡] and Stewart F. Parker*[,‡]

[†]School of Chemistry, Bangor University, Bangor, Gwynedd LL57 2UW, United Kingdom

[‡]ISIS Facility, STFC Rutherford Appleton Laboratory, Didcot, Chilton, Oxfordshire OX11 0QX, United Kingdom

Supporting Information

ABSTRACT: A structural, spectroscopic, and computational investigation of Stryker's reagent, $[HCu\{P(C_6H_5)_3\}]_6$, and its isotopomers has provided new insights into the complex. Neutron diffraction shows that the hydrides are best described as edge bridging rather than face bridging. The combination of infrared and inelastic neutron scattering spectroscopies has allowed the location of most of the modes associated with the hydrides and their assignments. The structural and spectroscopic conclusions are supported by the *ab initio* studies of the complex.

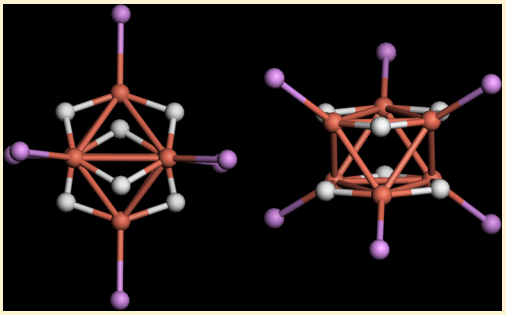

I. INTRODUCTION

In the late 1980s, J. M. Stryker and co-workers showed that the phosphine stabilized copper hydride hexamer, $[HCu\{P(C_6H_5)_3\}]_6$ (now known as Stryker's reagent), was able to regioselectively hydrogenate the alkene functionality of α,β-unsaturated ketones, esters, and aldehydes.[1] It has since been shown that it is possible to make the reaction catalytic in the reagent, which, combined with the mild reaction conditions, functional group compatibility, and excellent atom efficiency, has made this a highly versatile reagent.[2] By replacing the triphenylphosphine by a chiral phosphine, diastereo- and enantioselective reactions have been achieved.[3a−c] More recently, tandem cyclization reactions in one pot conversions have been demonstrated.[3d,e]

The complex has been structurally characterized by single crystal X-ray diffraction of the dimethyl formamide solvate[4] and neutron diffraction of the $P(C_6H_5CH_3)_3$ (=P(*p*-tolyl)$_3$) derivative.[5] Both studies found a distorted octahedron of copper atoms with six short (2.52 Å average) and six long (2.68 Å average) Cu−Cu edges, giving six small and two large faces, with each vertex capped by a phosphine ligand. In the X-ray study the hydrides were not located, but it was suggested that they were 2-fold bridging across the short edges.[4] The neutron diffraction study did locate the hydrides and described them as 3-fold bridging above the small faces.[5]

The hydrides may be observed with ^{1}H NMR spectroscopy,[6] but have not yet been detected by vibrational spectroscopy.[4] The aim of this Article is to characterize the hydrides in Stryker's reagent by a combination of vibrational spectroscopy, in particular inelastic neutron scattering spectroscopy,[7] and periodic density functional theory.

II. EXPERIMENTAL SECTION

A. Compounds. $[HCu\{P(C_6H_5)_3\}]_6$ was obtained from Aldrich (90%). $[DCu\{P(C_6H_5)_3\}]_6$ and $[HCu\{P(C_6D_5)_3\}]_6$ were made by variations on the method of Lee and Yun:[6]

$$6Cu(acetate)_2 + 6P(C_6H_5)_3 + 3(C_6H_5)_2SiH_2 \rightarrow [HCu\{P(C_6H_5)_3\}]_6 + 3(C_6H_5)_2Si(acetate)_2$$

$[DCu\{P(C_6H_5)_3\}]_6$ was made by using $(C_6H_5)_2SiD_2$ (Aldrich, 97% D) instead of $(C_6H_5)_2SiH_2$ and $[HCu\{P(C_6D_5)_3\}]_6$ using $P(C_6D_5)_3$ (Aldrich, 99% D) instead of $P(C_6H_5)_3$. A detailed, description of the procedure is given in the Supporting Information. ^{1}H NMR spectra (Bruker Advance III Ultrashield 400 at 400 MHz) of the compounds in C_6D_6 were in agreement with the literature,[6] in particular a peak at 3.51 ppm assigned to Cu−H was observed for $[HCu\{P(C_6H_5)_3\}]_6$ and $[HCu\{P(C_6D_5)_3\}]_6$ and absent in $[DCu\{P(C_6H_5)_3\}]_6$. The spectra are shown in the Supporting Information.

B. Vibrational Spectroscopy. The INS spectra were recorded using the high resolution (~1.25% $\Delta E/E$) broadband (−24 to 4000 cm^{-1}) spectrometer TOSCA[7,8] at the pulsed spallation neutron source ISIS[9] (Chilton, U.K.). TOSCA is an inverted geometry time-of-flight spectrometer where a pulsed, polychromatic beam of neutrons illuminates the sample at 17 m from the source. The scattered neutrons are Bragg reflected by a pyrolytic graphite analyzer, and after passage through a beryllium filter, only those with a final energy of ~32 cm^{-1} reach the ^{3}He detector bank; all others are Bragg scattered into the shielding. Energy transfer and spectral intensity are then calculated using standard programs to convert to $S(Q,\omega)$. The samples, 2−4 g, were loaded into aluminum sachets inside thin-walled indium sealed aluminum cans in an argon glovebox ([O_2], [H_2O] < 1 ppm), cooled to <10 K, and the spectra were recorded for 12 h for the $P(C_6H_5)_3$ containing samples and 48 h for $[HCu\{P(C_6D_5)_3\}]_6$. The INS spectra are available from the INS database at

Received: October 31, 2013
Published: February 26, 2014

http://wwwisis2.isis.rl.ac.uk/INSdatabase/. Infrared spectra (2 cm^{-1} resolution, 256 scans) were recorded with a Bruker Vertex 70 Fourier transform infrared spectrometer using a Specac Golden Gate variable temperature single reflection attenuated total internal reflection accessory.

C. Neutron Diffraction. Neutron diffraction measurements were carried out on the samples at room temperature using the SANDALS[10] diffractometer at ISIS.[9] For the measurements, the samples were loaded into 2 mm thick plate TiZr cells in the argon glovebox. Data reduction was carried out using the GUDRUN[11] package. Simulated radial distribution functions (rdf) were generated with PDFgui.[12]

D. *Ab Initio* Calculations. Periodic-DFT calculations were carried out using the plane wave pseudopotential method implemented in the CASTEP[13,14] code. Exchange and correlation were approximated using the PBE functional.[15] The plane-wave cutoff energy was 880 eV. Due to the size of the unit cell, Brillouin zone sampling of electronic states was performed on 1 × 1 × 1 Monkhorst-Pack grid. The equilibrium structure, an essential prerequisite for lattice dynamics calculations, was obtained by BFGS geometry optimization after which the residual forces were converged to zero within 0.0012 eV/A. Phonon frequencies were obtained by diagonalization of dynamical matrices computed using density-functional perturbation theory[16] (DFPT) and also to compute the dielectric response and the Born effective charges, and from these the mode oscillator strength tensor and infrared absorptivity were calculated. Transition energies for isotopic species were calculated from the dynamical matrix that is stored in the CASTEP checkpoint file using the PHONONS utility.[17] The atomic displacements in each mode that are part of the CASTEP output enable visualization of the modes to aid assignments and are also all that is required[7] to generate the INS spectrum using the program ACLIMAX.[18] While energy scaling is commonly used to improve the agrement between observed and calculated transition energies, we emphasize that all the calculated spectra shown here have *not* been energy scaled

III. RESULTS AND DISCUSSION

A. Structure. Two views of the $[HCuP]_6$ core of Stryker's reagent as determined by neutron diffraction[5] of the P(*p*-tolyl)$_3$

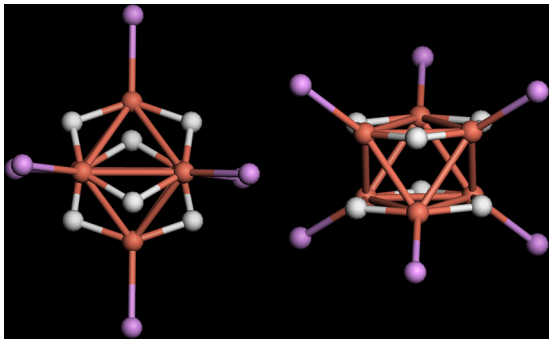

Figure 1. Two views of the $[HCuP]_6$ core of Stryker's reagent. The hydrides appear to be triply bridging and edge bridging, left and right view, respectively.

derivative are shown in Figure 1. In the structure on the left, the hydrides are seen to be triply bridging as asserted by the authors. However, in the structure on the right, the hydrides appear as edge bridging as suggested by the original X-ray diffraction study.[4] Inspection of the bond distances shows that for all three of the independent hydrides (the molecule occupies a C_i site in the crystal) two of the Cu−H distances are significantly shorter than the third: 1.72 and 1.73 vs 1.99 Å.

The Cu−H distances can be observed directly *via* the radial distribution function (rdf), $g(R)$, generated from neutron

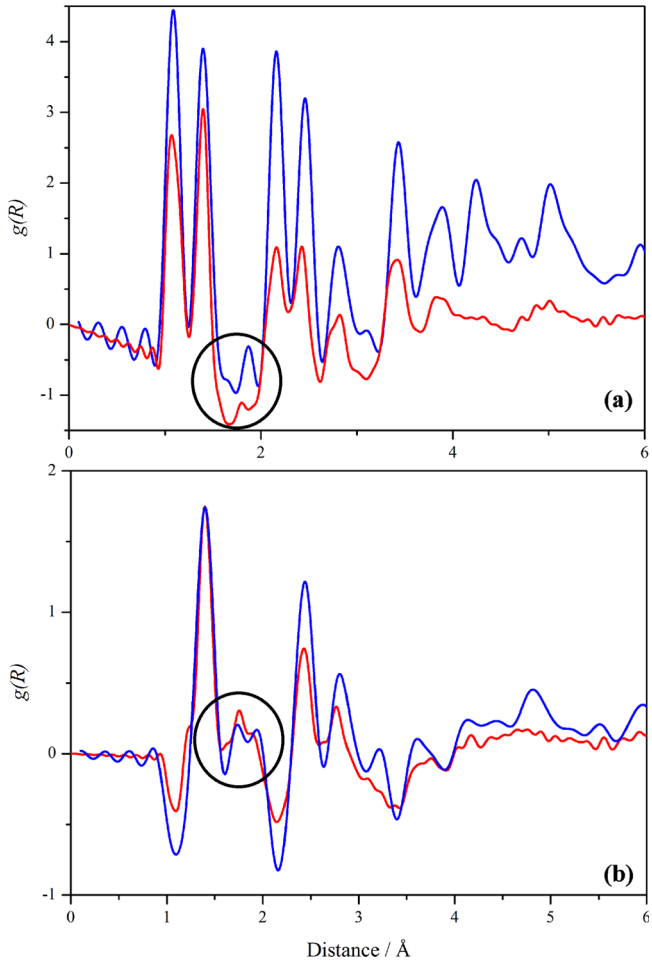

Figure 2. Observed (red traces) and calculated from the geometry optimized structure (blue traces) radial distribution functions of (a) $[HCu\{P(C_6H_5)_3\}]_6$ and (b) $[DCu\{P(C_6D_5)_3\}]_6$. The circled regions are where the Cu−H(D) features occur.

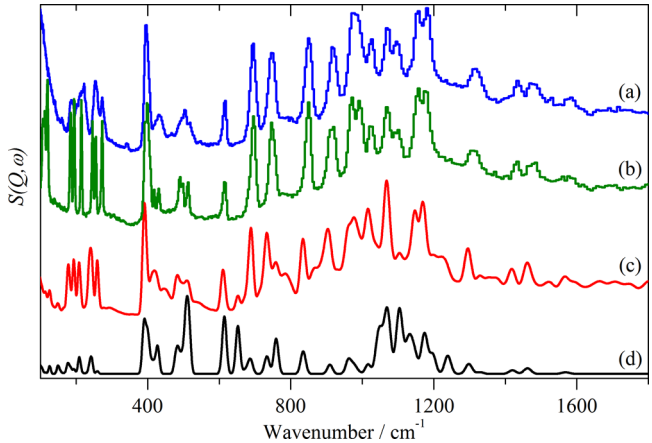

Figure 3. INS spectra of (a) $[HCu\{P(C_6H_5)_3\}]_6$ and (b) $P(C_6H_5)_3$. (c) INS spectrum of $[HCu\{P(C_6H_5)_3\}]_6$ generated from the CASTEP calculation and including all transitions 0−10. (d) Same as part c but only showing the 0−1 transitions that involve the hydrides. Note that the ordinate scales of parts c and d are not comparable.

diffraction data. Figure 2 shows the data (red traces). Hydrogen, ^1H, has a negative scattering length, whereas deuterium, carbon, phosphorus, and copper have positive scattering lengths. (A negative scattering length means that the

dx.doi.org/10.1021/ic402736t | Inorg. Chem. 2014, 53, 2963−2967

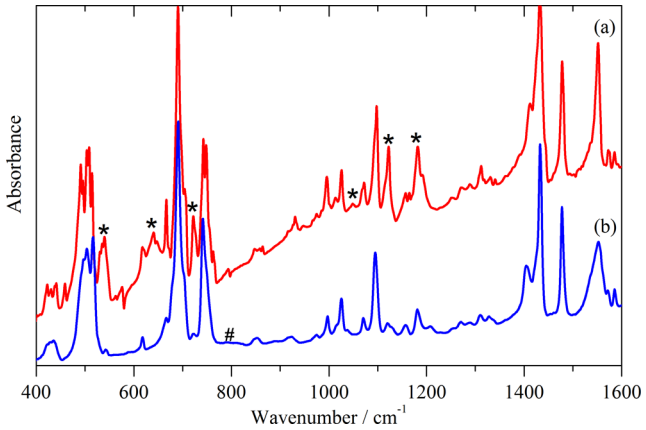

Figure 4. Infrared spectra at 115 K of (a) $[HCu\{P(C_6H_5)_3\}]_6$ and (b) $[DCu\{P(C_6H_5)_3\}]_6$. Asterisks (*) denote the position of Cu−H and the hash sign (#) Cu−D modes.

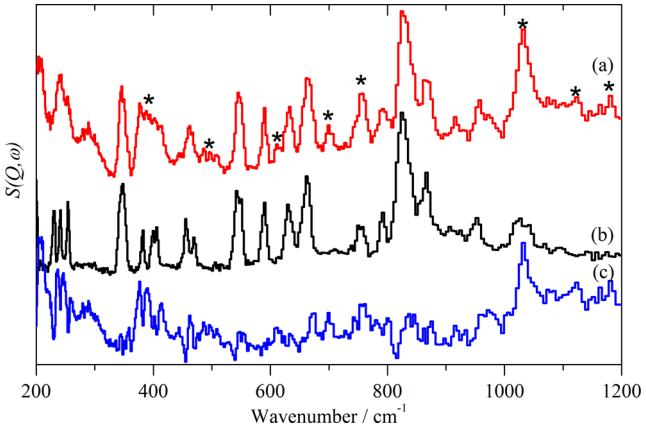

Figure 5. INS spectra at 20 K of (a) $[HCu\{P(C_6D_5)_3\}]_6$, (b) $P(C_6D_5)_3$, and (c) the scaled difference spectrum a − b. The ordinate scale in parts a and c is the same. Asterisks denote the position of Cu−H modes.

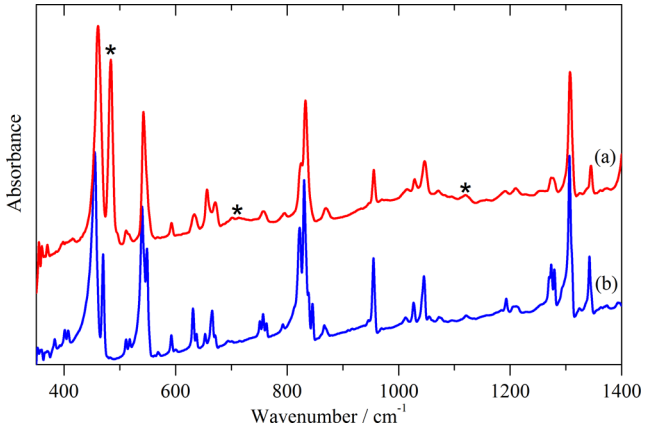

Figure 6. Infrared spectra at 115 K of (a) $[HCu\{P(C_6D_5)_3\}]_6$ and (b) $P(C_6D_5)_3$. Asterisks denote the position of Cu−H modes.

neutron undergoes a 180° phase shift on scattering.) Thus, negative-going features are distances that involve hydrogen. This is most clearly seen for the peak at 1.09 Å that is positive-going in Figure 2a and negative-going in Figure 2b due to the C−D and C−H of the phenyl ring in the triphenylphosphine ligand of $[HCu\{P(C_6D_5)_3\}]_6$ and $[DCu\{P(C_6H_5)_3\}]_6$, respectively, whereas the peak at 1.40 Å due to the C−C bond of the phenyl ring is positive-going in both parts a and b of Figure 2. The circled regions in Figure 2a,b correspond to the Cu−H and Cu−D distances, respectively, in the complex. Thus, in Figure 2a there are negative-going peaks at 1.67 and 1.92 Å, and in Figure 2b there are positive-going peaks at 1.75 and 1.89 Å, confirming the presence of two different Cu−H distances. Thus, the description of the hydrides as edge bridging is the better approximation; the hydrides are at most semiface bridging.

The distances we observe, Cu−H at 1.67 and 1.92 Å and Cu−D at 1.75 and 1.89 Å, are similar to those seen in the P(*p*-tolyl)$_3$ derivative:[5] 1.72, 1.73, and 1.99 Å. We estimate that the uncertainty in our distances is at most ±0.06 Å. Stevens et al.[5] considered that the *average* Cu−H distance of 1.76 Å was the most significant finding so that the hydrides were face bridging. The average distances from this work are Cu−H 1.75 Å and Cu−D 1.80 Å, very similar to the previous work. However, our data confirms the significance of the original neutron diffraction study,[5] which found two distinct Cu−H distances; thus, the hydrides are best described as edge-bridging in both the P(*p*-tolyl)$_3$ and the $P(C_6H_5)_3$ complexes.

The description as edge bridging is supported by *ab initio* calculations. The structure of the pure complex with $P(C_6H_5)_3$ ligands is not known (only as a solvate[4]), thus as an initial model for the system, we have used the neutron diffraction structure[5] of $[HCuP(p\text{-tolyl})_3]_6$ and replaced the methyl groups by hydrogen. The structure contains two independent molecules in the primitive cell, and both occupy inversion centers, one on the O-*a* edge and one in the *bc* plane resulting in a total of 416 atoms. In order to make the calculation tractable, we have retained the $P\bar{1}$ space group symmetry (and hence the inversion symmetry of the complex) and the experimental lattice parameters but removed the molecule on the O-*a* edge (and its periodic images). The vibrational spectroscopy shows no evidence for factor group splitting so it is reasonable to ignore the intermolecular interactions and treat the system as an isolated molecule. (The geometry optimized structure is given in the Supporting Information as a CIF file.) The rdfs calculated from the geometry optimized structures of the $[DCu\{P(C_6H_5)_3\}]_6$ and $[HCu\{P(C_6D_5)_3\}]_6$ are shown as the blue traces in Figure 2. Given the approximations in the model, the agreement is satisfactory and supports the description of the hydrides as largely edge bridging.

The calculations also give some insight into the bonding present. Our assumption was that it was Cu−Cu bonding that was responsible for the stability of the cluster. Inspection of the Mulliken populations suggests that there is in fact little Cu−Cu bonding present. The population of the short Cu−H bond is +0.38 electron (average), and that of the long Cu−H bond is +0.26 electron (average), so while the hydride is mainly edge-bridging, there is a significant interaction with the more distant Cu atom, and this contributes to the cluster's integrity.

B. Vibrational Spectroscopy. The $[HCuP]_6$ core of the *p*-tolyl derivative of Stryker's reagent has C_i symmetry, in the solid state. Thus, of the 18 modes resulting from the hydrides, half will be infrared active and half will be Raman active with no coincidences. As there are no selection rules in INS spectroscopy, all the modes are allowed in the INS spectrum. We are unaware of any studies on related systems; the most studied systems are the metal carbonyl hydrides, e.g.[19]

Figure 3a shows the INS spectrum of $[HCu\{P(C_6H_5)_3\}]_6$ and Figure 3b that of $P(C_6H_5)_3$. It can be seen that the

dx.doi.org/10.1021/ic402736t | Inorg. Chem. 2014, 53, 2963−2967

Table 1. Observed and Calculated CuH(D) Transition Energies

All H				CuH−(PPh_3−D_{15})				CuD−PPh_3			
expt/cm^{-1}		CASTEP		expt/cm^{-1}		CASTEP			CASTEP		
INS	IR	pos/ cm^{-1}	IR intensity/ km mol^{-1}	INS	IR	pos/ cm^{-1}	IR intensity/ km mol^{-1}	expt/ cm^{-1} IR	pos/ cm^{-1}	IR intensity/ km mol^{-1}	assignment
400		401	0	388		413	0		291	0	out-of-plane bend
		508	0	493		503	0		354	0	out-of-plane bend
	503/508	516	245	491	484	511	398		360	348	out-of-plane bend
619		616	135	613	633	614	151		441	76	out-of-plane bend
	641	652	36	700	705	658	18		462	29	out-of-plane bend
	748	760	0	756	757	760	0		538	0	out-of-plane bend
		1044	0	1032		1044	0		743	0	symmetric stretch
	1048	1052	455			1053	447		750	239	asymmetric stretch
		1064	0			1068	0		760	0	symmetric stretch
		1070	88	1081		1074	450		767	247	symmetric stretch
		1099	41			1099	40	791	780	30	asymmetric stretch
		1107	0			1106	0		788	0	symmetric stretch
	1114	1107	60			1107	59	806	784	37	asymmetric + symmetric stretch
1126	1122	1126	42	1122	1121	1126	41	821	798	25	asymmetric + symmetric stretch
		1136	0			1136	0		805	0	symmetric stretch
		1177	0	1185		1177	0		834	0	asymmetric stretch
	1192	1197	0			1197	0		849	0	asymmetric stretch
		1239	5			1239	5		880	2	asymmetric stretch

spectrum is completely dominated by the vibrations of the phosphine ligand. This is as expected since INS intensities are directly proportional to the number of scatterers; thus, the ratio of intensities is 90:6 for phosphine:hydride. To aid in the detection of the modes we have calculated the INS and infrared spectra of the three complexes. Figure 3c shows the calculated INS spectrum of the complex. The agreement is excellent; however, it is also dominated by motions of the phosphine. To generate the INS spectrum, the ACLIMAX program[18] calculates the amplitude of vibration of each atom from its displacement in each mode; the displacement is weighted by the total scattering cross section. If the cross sections of all the atoms are set to zero, except for the atoms of interest, then the result shows which atoms have significant motion in each mode. Figure 3d shows the case where only the hydrides bonded to copper retain any cross section. The regions that have the largest contribution from the hydrides are 400−500, ∼600, and 1000−1200 cm^{-1}. A 2-fold bridging hydride has an out-of-plane bend and symmetric and asymmetric stretches; hence the six out-of-plane bend modes occur in the 400−600 cm^{-1} region, and the 12 stretch modes occur in the 1000−1200 cm^{-1} region. However, there is also intensity outside of these regions indicating that at least some of the modes mix with adjacent phosphine modes.

The classical method for the detection of hydride modes is to compare the spectra of the hydride and deuteride. For the metal carbonyl hydrides,[19b−d] this procedure is aided by recording the spectra at low temperature, where the hydride (deuteride) modes undergo a marked sharpening. Figure 4 compares the infrared spectra at 115 K of $[HCu\{P(C_6H_5)_3\}]_6$ (Figure 4a) and $[DCu\{P(C_6H_5)_3\}]_6$ (Figure 4b). While the spectra are generally sharper at 115 K than at room temperature, there are no major changes. The only exception is the band at 641 cm^{-1} that is more intense at 115 K. Close inspection reveals a number of bands that are present in the hydride infrared spectrum but not that of the deuteride. These are marked by an asterisk. It would be expected that some of the bands would show deuterium counterparts; the only new feature that occurs is at 791 cm^{-1} (marked by #). The other bands are not observed either because of accidental overlap with phosphine modes or that they are shifted below the instrumental limit of 400 cm^{-1}.

Comparison of the corresponding INS spectra of $[HCu\{P(C_6H_5)_3\}]_6$ and $[DCu\{P(C_6H_5)_3\}]_6$ is not informative as the spectra are dominated by the phosphine modes (see Supporting Information, Figure S4). The interference from the phosphines can be dramatically reduced by deuteration of the phosphines. In this event the relative intensities of the phosphine and the hydride become approximately equal because the cross section of deuterium is ∼1/20 that of hydrogen ^1H, thus compensating for their greater number. Figure 5a shows the INS spectrum of $[HCu\{P(C_6D_5)_3\}]_6$, Figure 5b that of $P(C_6D_5)_3$, and Figure 5c the scaled difference spectrum. The hydride modes are marked by an asterisk in Figure 5a. Note that the difference spectrum, Figure 5c, should resemble the "Cu−H only" spectrum of the parent compound, Figure 3d, and this is seen to be case. (Figure S5 of the Supporting Information shows the direct comparison.) Figure 6 shows the corresponding infrared spectra of $[HCu\{P(C_6D_5)_3\}]_6$, part a, and that of $P(C_6D_5)_3$, part b, at 115 K. In addition to two weak modes there is also a very strong mode at 491 cm^{-1}.

Table 1 lists the observed and calculated transition energies for all three isotopomers. Visualization of the modes as calculated by CASTEP allows assignments, and these are also given. As with the metal carbonyl hydrides[19b−d] the modes follow the order asymmetric stretch > symmetric stretch > out-of-plane bend. However, unlike the metal carbonyl hydrides there is much less distinction between the transition energies of the asymmetric and symmetric modes, and some modes have a mixture of both types of motion.

dx.doi.org/10.1021/ic402736t | Inorg. Chem. 2014, 53, 2963−2967

IV. CONCLUSIONS

A combination of inelastic neutron scattering and infrared spectroscopies combined with *ab initio* calculations has enabled the identification of the spectral features that contain significant contributions from Cu−H stretch and bend modes. The use of Stryker's reagent and its derivatives is an active area of synthetic organic chemistry.[2,3] Infrared spectroscopy is a convenient method to follow reactions *in situ*, but it depends on having reliable assignments for the species of interest. This work provides such assignments for the active element of Stryker's reagent.

■ ASSOCIATED CONTENT

Ⓢ Supporting Information

Detailed, illustrated description of the synthetic procedure. Solution ^{1}H NMR spectra of the three compounds. CIF data of the geometry optimized structure of Stryker's reagent. This material is available free of charge via the Internet at http://pubs.acs.org.

■ AUTHOR INFORMATION

Corresponding Author

*E-mail: stewart.parker@stfc.ac.uk.

Notes

The authors declare no competing financial interest.

■ ACKNOWLEDGMENTS

We thank the STFC Rutherford Appleton Laboratory for access to neutron beam facilities. Computing resources (time on the SCARF computer used to perform the CASTEP calculations) were provided by STFC's e-Science facility.

■ REFERENCES

(1) (a) Mahoney, W. S.; Brestensky, D. M.; Stryker, J. M. *J. Am. Chem. Soc.* **1988**, *110*, 291−293. (b) Brestensky, D. M.; Huseland, D. E.; McGettigan, C.; Stryker, J. M. *Tetrahedron Lett.* **1988**, *29*, 3749−3752. (c) Brestensky, D. M.; Stryker, J. M. *Tetrahedron Lett.* **1989**, *30*, 5677−5680. (d) Koenig, T. M.; Daeuble, J. F.; Brestensky, D. M.; Stryker, J. M. *Tetrahedron Lett.* **1990**, *31*, 3237−3240.

(2) Deutsch, C.; Krause, N.; Lipshutz, B. H. *Chem. Rev.* **2008**, *108*, 2916−2927.

(3) (a) Schmid, R.; Broger, E. A.; Cereghetti, M.; Crameri, Y.; Foricher, J.; Lalonde, M.; Muller, R. K.; Scalone, M.; Schoettel, G.; Zutter, U. *Pure Appl. Chem.* **1996**, *68*, 131−138. (b) Saito, T.; Yokozawa, T.; Ishizaki, T.; Moroi, T.; Sayo, N.; Miura, T.; Kumbayashi, T. *Adv. Synth. Catal.* **2001**, *343*, 264−267. (c) Blaser, H.-U.; Brieden, W.; Pugin, B.; Spindler, F.; Studer, M.; Togni, A. *Top. Catal.* **2002**, *19*, 3−19. (d) Sass, D. C.; de Lucca, E. C., Jr.; da Silva Barbosa, J.; de Oliveira, K. T.; Constantino, M. G. *Tetrahedron Lett.* **2011**, *52*, 5371−5374. (e) Sass, D. C.; Heleno, V. C. G.; Lopes, J. L. C.; Constantino, M. G. *Tetrahedron Lett.* **2008**, *49*, 3877−3880.

(4) Churchill, M. R.; Bezman, S. A.; Osborn, J. A.; Wormald, J. *Inorg. Chem.* **1972**, *11*, 1818.

(5) Stevens, R. C.; McLean, M. R.; Bau, R.; Koetzle, T. F. *J. Am. Chem. Soc.* **1989**, *111*, 3472−3473.

(6) Lee, D.-W.; Yun, J. *Tetrahedron Lett.* **2005**, *46*, 2037−2039.

(7) Mitchell, P. C. H.; Parker, S. F.; Ramirez-Cuesta, A. J.; Tomkinson, J. *Vibrational Spectroscopy with Neutrons: With Applications in Chemistry, Biology, Materials Science, and Catalysis*; World Scientific: Singapore, 2005.

(8) Colognesi, D.; Celli, M.; Cilloco, F.; Newport, R. J.; Parker, S. F.; Rossi-Albertini, V.; Sacchetti, F.; Tomkinson, J.; Zoppi, M. *Appl. Phys. A: Mater. Sci. Process.* **2002**, *74*, S64.

(9) www.isis.stfc.ac.uk.

(10) http://www.isis.stfc.ac.uk/instruments/sandals/.

(11) http://www.isis.stfc.ac.uk/instruments/sandals/data-analysis/gudrun8864.html.

(12) Farrow, C. L.; Juhás, P.; Liu, J. W.; Bryndin, D.; Božin, E. S.; Bloch, J.; Proffen, Th.; Billinge, S. J. L. *J. Phys.: Condens. Matter* **2007**, *19*, 335219.

(13) Clark, S. J.; Segall, M. D.; Pickard, C. J.; Hasnip, P. J.; Probert, M. J.; Refson, K.; Payne, M. C. *Z. Kristallogr.* **2005**, *220*, 567.

(14) Refson, K.; Tulip, P. R.; Clark, S. J. *Phys. Rev. B* **2006**, *73*, 155114.

(15) Perdew, J.; Burke, K.; Ernzerhof, M. *Phys. Rev. Lett.* **1996**, *77*, 3865.

(16) Milman, V.; Perlov, A.; Refson, K.; Clark, S. J.; Gavartin, J.; Winkler, B. *J. Phys.: Condens. Matter* **2009**, *21*, 485404.

(17) Refson, K. *Phonons and Related Calculations in CASTEP*; http://www.castep.org/.

(18) Ramirez-Cuesta, A. J. *Comput. Phys. Commun.* **2004**, *157*, 226.

(19) (a) *Transition Metal Hydrides*; Bau, R., Ed.; Advances in Chemistry 167; American Chemical Society: Washington, DC, 1978. (b) Andrews, J. R.; Kettle, S. F. A.; Powell, D. B.; Sheppard, N. *Inorg. Chem.* **1982**, *21*, 2874−2877. (c) Howard, M. W.; Skinner, P.; Bhardwaj, R. K.; Jayasooriya, U. A.; Powell, D. B.; Sheppard, N. *Inorg. Chem.* **1986**, *25*, 2846−2850. (d) Anson, C. E.; Jayasooriya, U. A.; Kettle, S. F. A.; Stanghellini, P. L.; Rossetti, R. *Inorg. Chem.* **1991**, *30*, 2282−2286. (e) Eckert, J.; Albinati, A.; Longoni, G. *Inorg. Chem.* **1989**, *28*, 4055−4056.